

Optical Depth Effects on the Formation of Spectral Lines in Rotating and Expanding Spherical Atmospheres

A. Peraiah, G. Raghunath and K. N. Nagendra *Indian Institute of Astrophysics, Bangalore 560034*

Received 1981 April 15; accepted 1981 August 27

Abstract. We have investigated the effects of increasing optical depths on spectral lines formed in a rotating and expanding spherical shell. We have assumed a shell whose outer radius is 3 times the inner radius, with the radial optical depths equal to 10, 50, 100, 500. We have employed a constant velocity with no velocity gradients in the shell. The shell is assumed to be rotating with velocities varying as $1/\rho$, where ρ is the perpendicular distance from the axis of rotation, implying the conservation of angular momentum. Two expansion (radial) velocities are treated: (1) $V = 0$ (static case) and (2) $V = 10$ mean thermal units. The maximum rotational velocities are $V_{\text{rot}} = 0, 5, 10$ and 20. In the shell where there are no radial motions, we obtain symmetric lines with emission in the wings for $V_{\text{rot}} = 0$ and 5 while for $V_{\text{rot}} \geq 10$ we obtain symmetric absorption lines. In the case of an expanding shell, we obtain lines with central emission.

Key words: spectral lines—rotating and expanding shells

1. Introduction

In an earlier paper (Peraiah 1980, henceforth called Paper I) we have investigated how rotation affects the line profiles formed in radially expanding atmospheres. There we have treated small rotational velocities with a constant optical thickness and found out that there are substantial changes introduced by rotation and radial expansion. However, in reality, there are stars whose atmospheres rotate faster and simultaneously expand radially (Slettebak 1979). Here we intend to study how high optical depths and large rotational velocities change the spectral lines observed at infinity in a shell of varying optical thickness.

2. The model and the computational procedure

First, we shall give a brief account of the model we have chosen. The main purpose of this investigation is to study the effects of a rotating and radially expanding shell on the formation of lines in it. Therefore, we have chosen a shell whose inner and outer radii are

$$r_{\text{in}} = 2.6 \times 10^{11} \text{ cm},$$

$$r_{\text{out}} = 3 \times 10^{11} \text{ cm}$$

while the radius of the star is

$$r_* = 10^{11} \text{ cm}.$$

The intermediate space between the shell and the star is assumed to have a continuous distribution of matter, *i.e.* there is no discontinuity in density. The density is adjusted in such a way that most of the matter is concentrated in the shell. Here we should realize that the equation of continuity need not apply for a spherically symmetric steady-state flow, because of the time dependency. Due to this uncertainty, we assumed densities in the shell which would give us radial optical depths of 10, 50, 100 and 500. We have shown the shell in Fig. 1. We have divided the medium of 4×10^{10} cm into a large number of shells smaller in size so that it is convenient to calculate the solution. The emergent rays are calculated along the line of sight. The emergent intensity in each shell is obtained from the formal solution of radiative transfer and is given by (see Mihalas 1978)

$$I(\tau_1, \mu, x) = I(\tau_2, \mu, x) \exp [-(\tau_2 - \tau_1)/\mu] + \int_{\tau_1}^{\tau_2} S(t) \exp [-(t - \tau_1)/\mu] dt/\mu, \quad (1)$$

where x is the normalized frequency given as $x = (\nu - \nu_0)/\Delta_s$ (Δ_s being a standard frequency interval), τ_1, τ_2 are the optical depths (at the boundaries of a small shell) along the line of sight, τ_2 being away from the observer (see Fig. 1). In general, μ is the cosine of the angle made by the ray with the line of sight and $S(t)$ is the source function. Here we are considering the rays along the line of sight and therefore μ is kept equal to 1. I is the specific intensity. Hence equation (1) becomes

$$I(\tau_1, x) = I(\tau_2, x) \exp [-(\tau_2 - \tau_1)] + \int_{\tau_1}^{\tau_2} S(t) \exp [-(t - \tau_1)] dt. \quad (2)$$

We have assumed a source function that varies as $1/r^2$. The optical depths in equations (1) and (2) are calculated along the line of sight. The difference $\tau_2 - \tau_1$ is calculated as this is the quantity that enters the calculation of emergent intensities. This is given by

$$\tau_2 - \tau_1 = K_0 N \exp (-x'^2) \Delta Q, \quad (3)$$

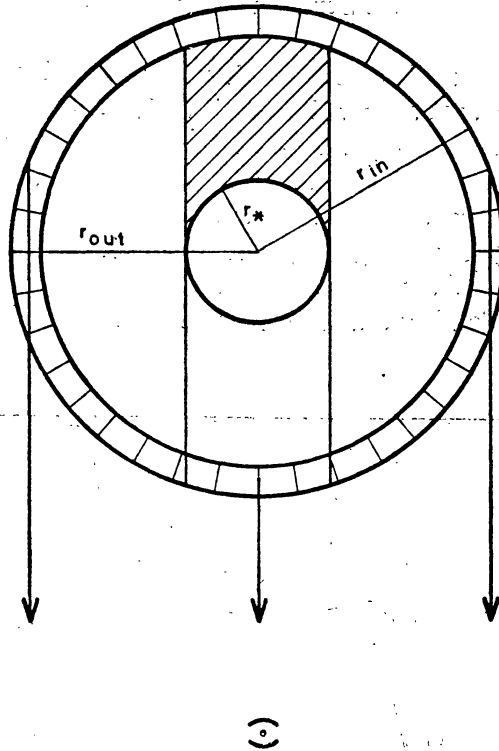


Figure 1. Schematic diagram of the shell.

where ΔQ is the geometrical distance along the line of sight between two consecutive shell boundaries. N is the density of the atoms in the shell. K_0 is the absorption coefficient. This quantity is chosen in such a way that the radial optical depths are 10, 50, 100 and 500. The quantity x' is the normalized frequency which is given by

$$x' = x + \mathbf{V}_{\text{rot}} \cdot \mathbf{l} + \mathbf{V}_{\text{rad}} \cdot \mathbf{l}, \quad (4)$$

where \mathbf{l} is the unit vector in the line of sight and \mathbf{V}_{rot} and \mathbf{V}_{rad} are the rotational and radial velocities. \mathbf{V}_{rot} and \mathbf{V}_{rad} are normalized in terms of mean thermal velocity units (mtu). The integral in equation (2) has been evaluated by assuming that the source function S changes linearly with respect to $(\tau_2 - \tau_1)$ between the two successive shell boundaries along the line of sight (radial variation of S should not be misunderstood with its variation along the line of sight). No incident radiation has been given from outside the shell. The emergent intensities are calculated for each of the smaller shells by employing equation (2) and this process is repeated until the emergent intensity at the final shell is obtained. The flux is calculated by the relation

$$F_x = 2\pi \int_{r_*}^{r_{\text{out}}} I(h, x) h dh, \quad (5)$$

where h is the perpendicular distance from the centre of the star to the ray parallel to the line of sight.

3. Discussion of the results

The results are presented in Figs 2-9. We have considered two cases: (1) a rotating but static shell and (2) a rotating and expanding shell. The velocity of expansion in the second case is taken to be equal to 10 mtu (all velocities are measured in mtu and henceforth we omit the units). The rotational velocities are assumed to vary according to the principle of conservation of angular momentum. Therefore, we set them to change proportionately according to $1/\rho$ where ρ is the perpendicular distance from the rotation axis. Essentially, we calculate the flux in the cylindrical tubes with the line of sight as axis which is parallel to the rotation axis. The maximum rotational

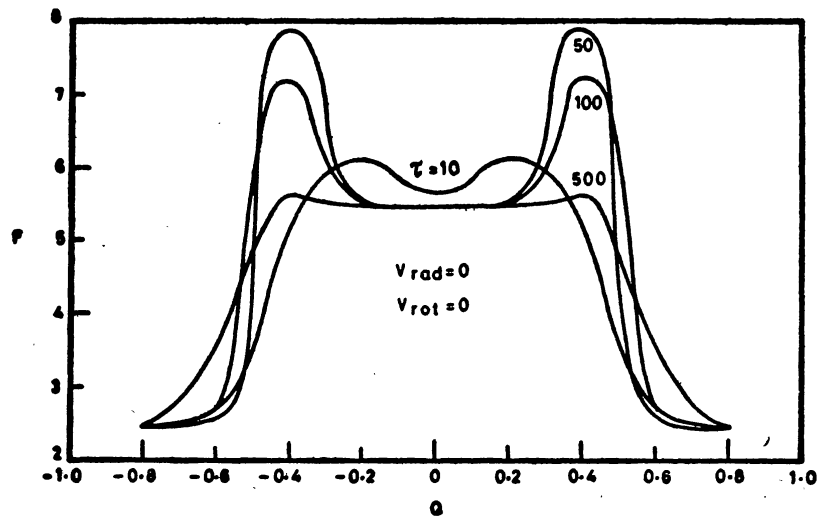


Figure 2. Line profiles for $V_{\text{rad}} = 0$, $V_{\text{rot}} = 0$; $F = F(x)/F(x_{\text{max}})$; $Q = x/x_{\text{max}}$.

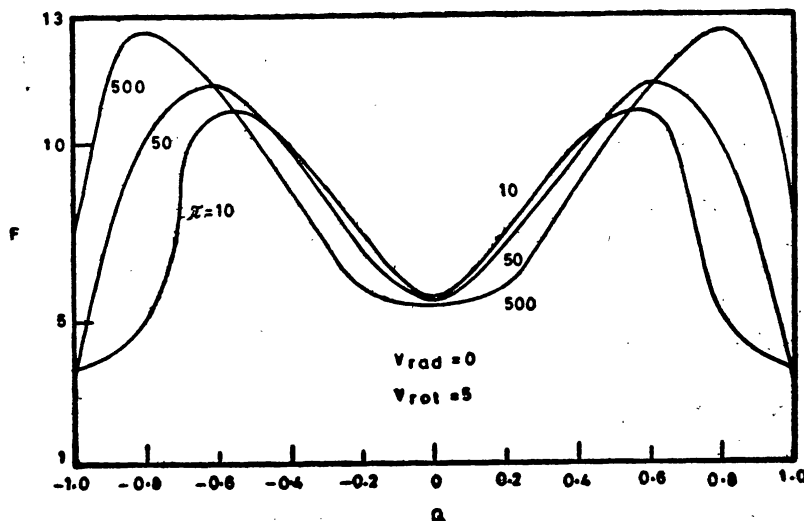


Figure 3. Line profiles for $V_{\text{rad}} = 0$, $V_{\text{rot}} = 5$.

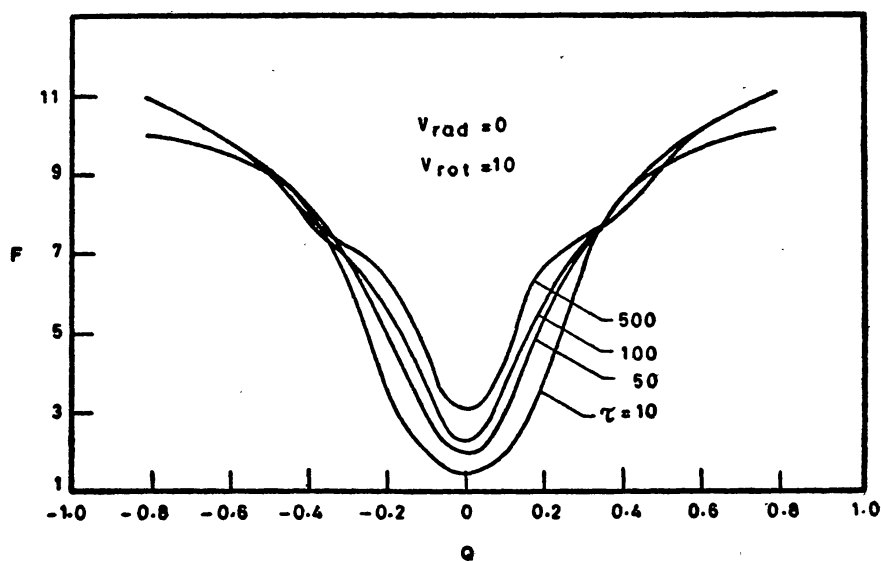


Figure 4. Line profiles for $V_{\text{rad}} = 0$, $V_{\text{rot}} = 10$.

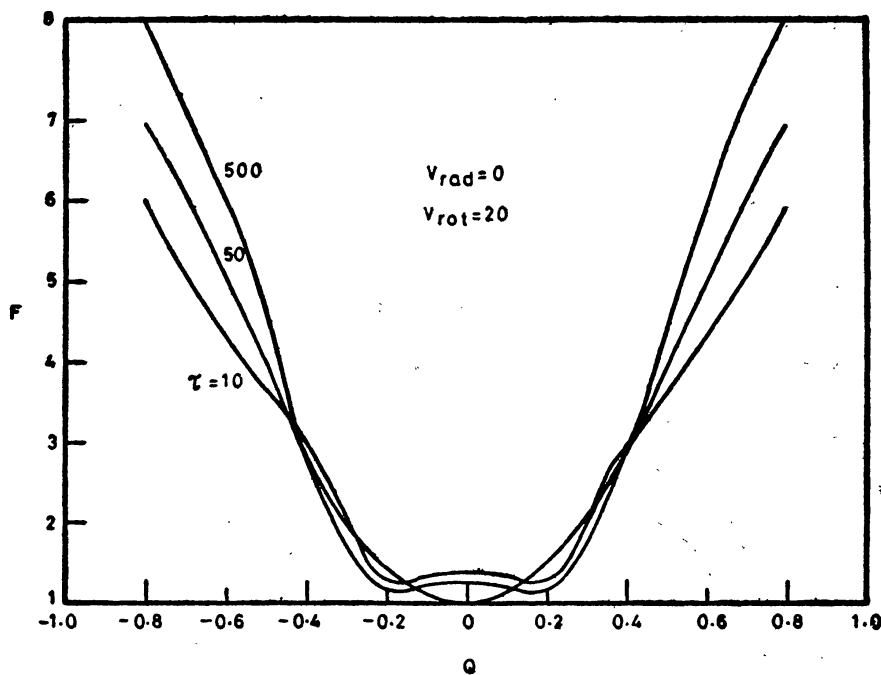
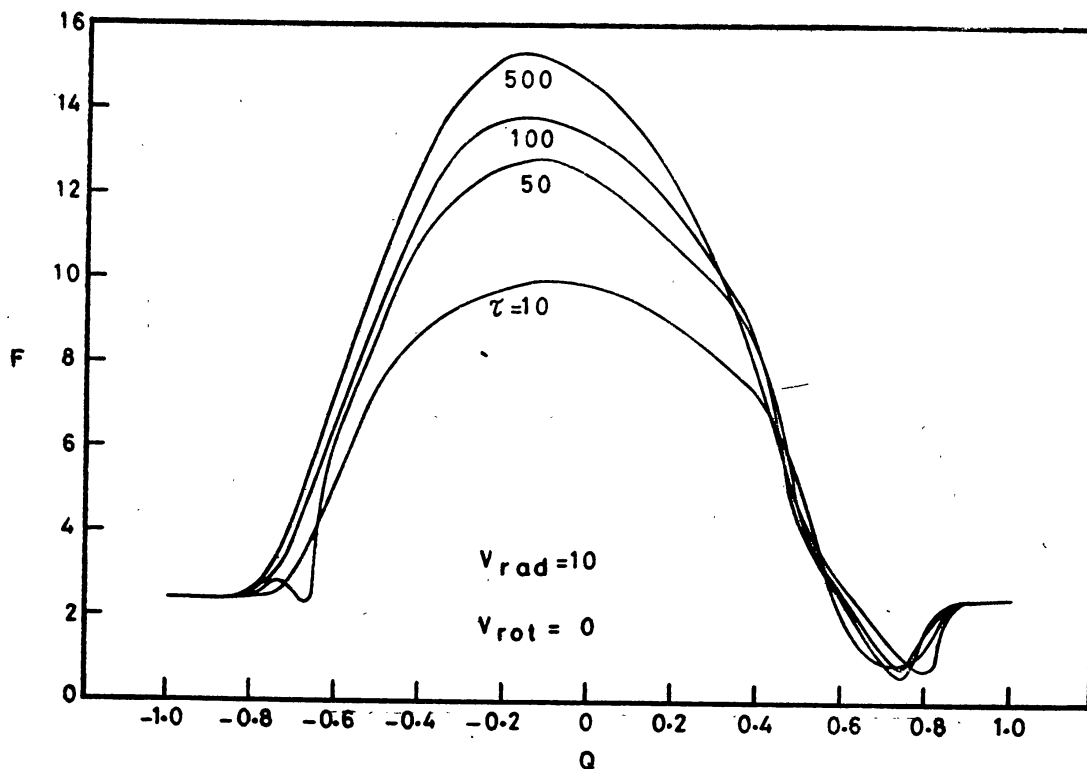
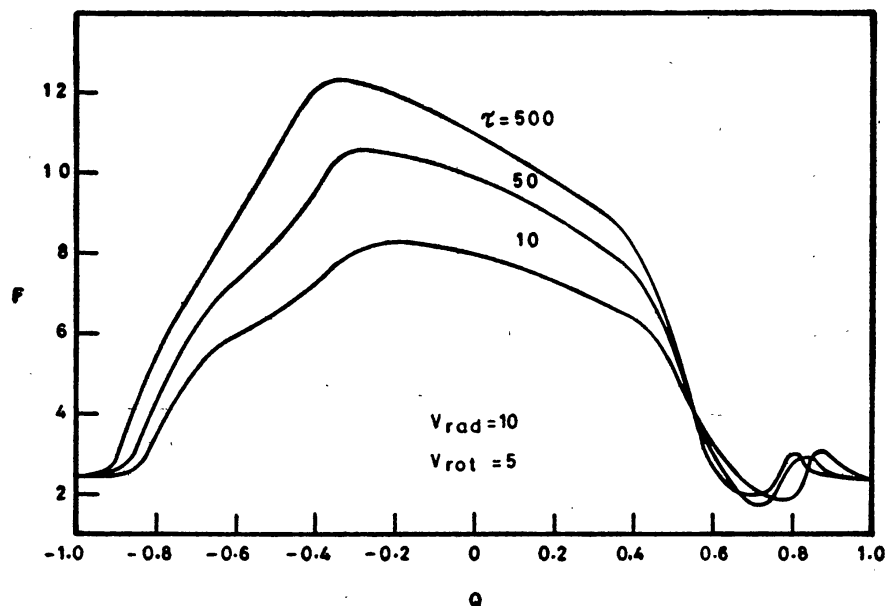


Figure 5. Line profiles for $V_{\text{rad}} = 0$, $V_{\text{rot}} = 20$.

velocity at r_* is taken to be 0, 5, 10 and 20 corresponding to Figs 2, 3, 4 and 5 respectively. We have plotted in these figures the ratio of $F = F(x)/F(x_{\text{max}})$ to $Q = x/x_{\text{max}}$. The profiles in Fig. 2 are in emission and symmetrical about the centre of the line with central absorption. As the optical depth increases the emission in the wings also increase with almost a proportionate decrease in the central absorption. In Fig. 3, we present results for $V_{\text{rad}} = 0$ and $V_{\text{rot}} = 5$. As one would expect, the lines become broader, but exhibit essentially the same profile. In Fig. 4, the lines

Figure 6. Line profiles for $V_{\text{rad}} = 10$, $V_{\text{rot}} = 0$.Figure 7. Line profiles for $V_{\text{rad}} = 10$, $V_{\text{rot}} = 5$.

are given for $V_{\text{rad}} = 0$ and $V_{\text{rot}} = 10$. There is a dramatic change in the profiles. The emission from the wings disappears completely and a pure symmetric absorption line appears. When V_{rot} is further increased to 20, symmetric absorption lines appear with broadened profiles (see Fig. 5).

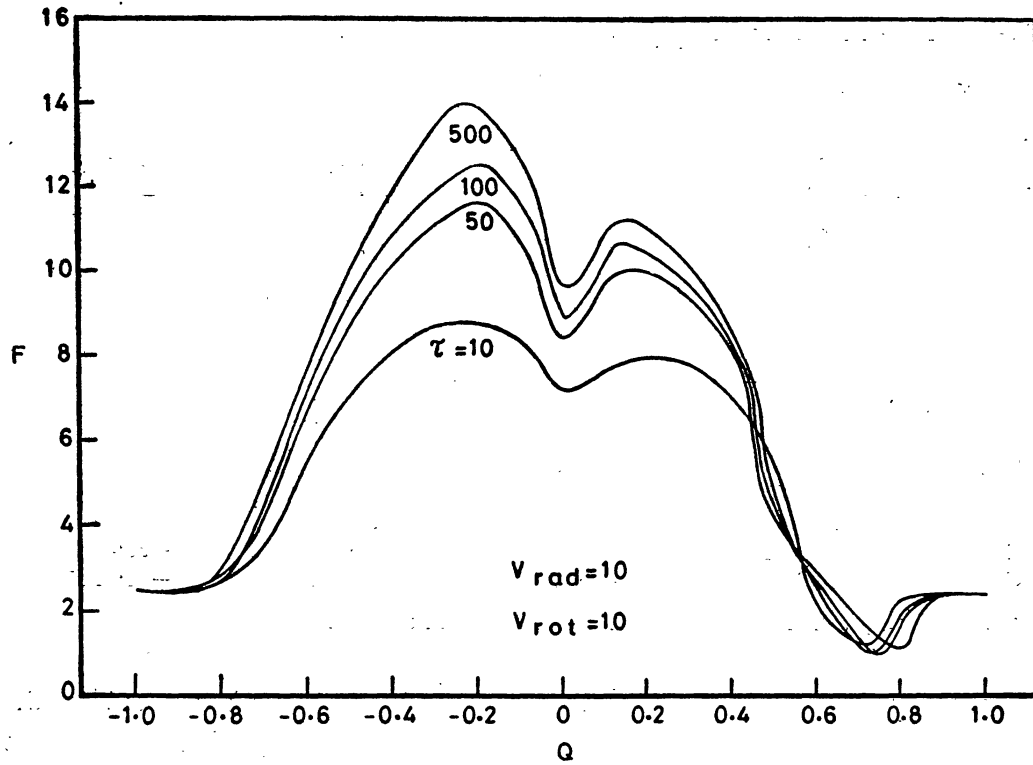
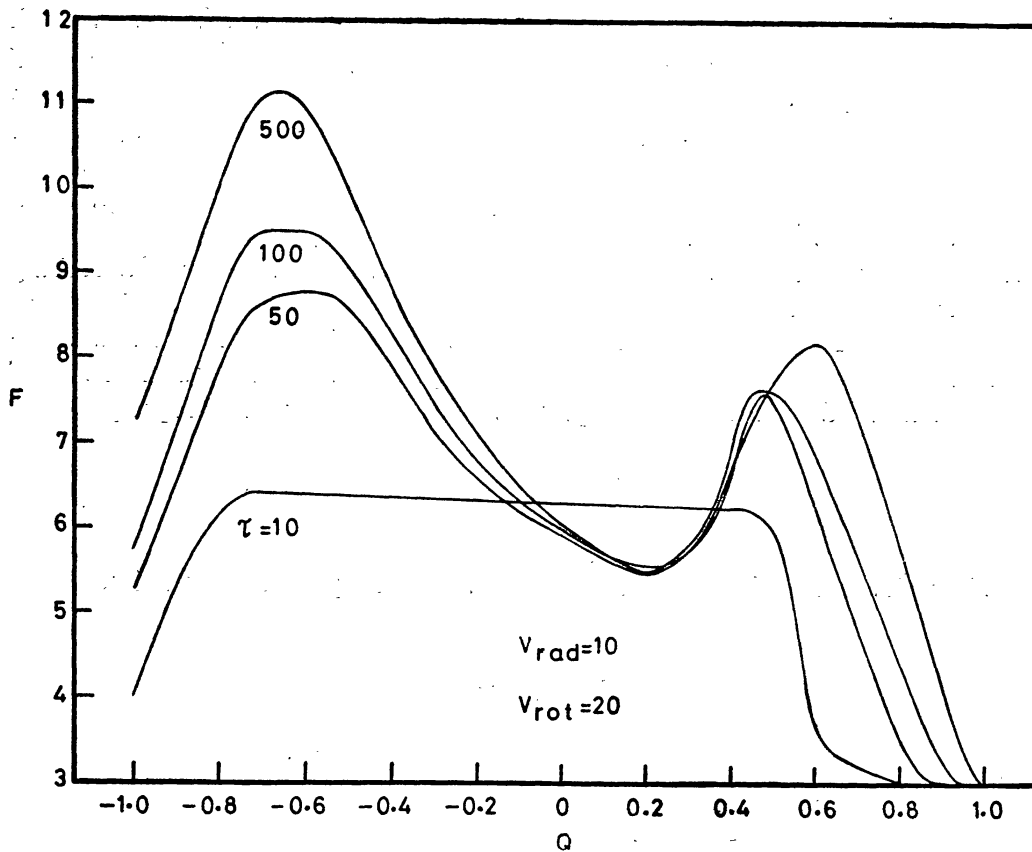
Figure 8. Line profiles for $V_{\text{rad}} = 10$, $V_{\text{rot}} = 10$.Figure 9. Line profiles for $V_{\text{rad}} = 10$, $V_{\text{rot}} = 20$.

Table 1. Equivalent widths for $V_{\text{rad}} = 0$.

| τ | 10 | 50 | 100 | 500 |
|------------------|----------|----------|--------|---------|
| V_{rot} | | | | |
| 0 | -6.6283 | -8.2914 | -7.799 | -7.7712 |
| 5 | -37.2515 | -16.1857 | -5.944 | -2.4224 |
| 10 | -2.702 | 3.2478 | 3.1773 | 2.8508 |
| 20 | 5.2665 | 5.2844 | 5.24 | 4.8836 |

Note: Negative equivalent widths mean that the lines are in emission.

Table 2. Equivalent widths for $V_{\text{rad}} = 10$.

| τ | 10 | 50 | 100 | 500 |
|------------------|----------|----------|----------|----------|
| V_{rot} | | | | |
| 0 | -40.6318 | -55.603 | -60.1595 | -66.7998 |
| 5 | -37.2515 | -50.3248 | -54.5 | -60.75 |
| 10 | -33.9622 | -44.7707 | -42.7826 | -53.43 |
| 20 | -10.5504 | -7.3345 | -5.982 | -1.3147 |

Note: Negative equivalent widths mean that the lines are in emission.

A constant velocity of $V_{\text{rad}} = 10$ and $V_{\text{rot}} = 0, 5, 10$ and 20 were introduced into the shell and these results are presented in Figs 6 to 9 respectively. The line profiles shown in Fig. 6 show emission and a small absorption in the blue side (about 7 per cent). The lines are asymmetric because of the expansion velocities. When the rotational velocity is increased to 5 then the asymmetry in the profiles increases. With $V_{\text{rot}} = 10$, again we note that there is a central absorption whose minimum is exactly at $Q = 0$ (see Fig. 8). A further increase in the rotational velocity to 20, changes the line profiles to those with asymmetric emission wings. It is interesting to note how the optical depths change the profiles. Although the optical depths do not change the profiles of the lines substantially, the equivalent widths are affected considerably (see Tables 1 and 2).

These results do show that the rotation, expansion and the number of absorbing atoms (through the changes in the optical depth) give rise to considerable changes in the line profiles. Therefore, one has to incorporate all such effects mentioned above in simulating the observed line profiles. One might obtain erroneous estimates of mass losses if one does not take these physical effects into account properly.

Acknowledgement

The authors thank the referees for pointing out a few conceptual discrepancies.

References

- Mihalas, D. 1978, *Stellar Atmospheres*, 2nd edn, Freeman, San Francisco.
 Peraiah, A. 1980, *J. Astrophys. Astr.*, **1**, 17 (Paper I).
 Slettebak, A. 1979, *Space Science Rev.*, **23**, 541.